Bipolar resistive switching characteristics of low temperature grown ZnO thin films by plasma-enhanced atomic layer deposition

Jian Zhang,[1)] Hui Yang,[1)] Qi-long Zhang,[1, a)] Shurong Dong,[2, a)] J.K.Luo[2, 3)]

[1]Department of Materials Science and Engineering, Zhejiang University, Hangzhou 310027, China
[2]Department of Information Science and Electronic Engineering, Zhejiang University, Hangzhou 310027, China
[3]Institute of Renewable Energy & Environmental Technology, Bolton University, Deane Road, Bolton, BL3 5AB, UK

ZnO films deposited by plasma-enhanced atomic layer deposition (PEALD) have been used to investigate resistive memory behavior. The bipolar resistance switching properties were observed in the Al/PEALD-ZnO/Pt devices. The resistance ratio for the high and low resistance states (HRS/LRS) is more than 10^3, better than that of other ZnO devices deposited by other methods. The dominant conduction mechanisms of HRS and LRS are trap-controlled space charge limited current and Ohmic behavior, respectively. The resistive switching behavior is induced upon the formation/disruption of conducting filaments. This study demonstrated that the PEALD-ZnO films have better properties for the application in 3D resistance random access memory.

Bipolar resistive switching (BRS) behaviors in transition-metal oxides (TMO) has been intensively studied as the next generation nonvolatile resistance random access memory (ReRAM).[1,2] The BRS behavior originates from the repeated resistance change between the high resistance state (HRS) and low resistance state (LRS), and is controlled by electric field with

[a] Electric mail: mse237@zju.edu.cn; dongshurong@zju.edu.cn

opposite polarity.[3] The resistive switching behaviors were observed from various binary TMO thin films such as NiO, TiO_2, ZnO and others.[4-6] This type of memory devices, generally composed of metal-insulator-metal structures, have many merits for applications such as high-density, high-speed and low-power consumption.

Owing to its direct energy band gap and abundance of the raw material, ZnO is an important material, ideally suited for applications in optoelectronics and electronics. Recent researches have shown that ZnO-based thin films have good resistive switching characteristics as well and are very promising for ReRAM application. BRS characteristics have been observed in TiN/ZnO/Pt, Ag/ZnO/Pt, Cr/ZnO/Pt, Al/ZnO/Pt and Al/ZnO/Si devices.[6-8] Most of the ZnO films were deposited by physical vapor-phase deposition (PVD) method, especially the magnetron sputtering. There has been limited activity in using chemical vapor-phase deposited (CVD) ZnO films to make the resistive switching devices. Atomic layer deposition (ALD), a special CVD technique, has potential benefits for high quality ZnO deposition owing to precise thickness controllability, large area uniformity, and low process temperature.[9] ALD is much better for electronic applications, especially when the films are extremely thin in nanometers range. Furthermore, ALD growth has a high conformality which is particularly suitable for 3D memories constructed in the cross-bar architecture.[10] Therefore, it is of great interest to investigate whether ZnO thin films grown by ALD can be used for ReRAM application.

In this paper, we report the BRS behaviors in undoped ZnO polycrystalline films deposited by a remote plasma-enhanced ALD (PEALD) method. By using remote PEALD, the defects associated with the plasma damage can be minimized.[11] Although ZnO films can also be grown by thermal ALD (THALD),[12] the resistivity of THALD-grown ZnO films is typically very low (<10 Ω•cm) due to high carrier concentration induced by oxygen vacancies, hence are not suitable for BRS device fabrication. Whereas the resistivity of the PEALD-grown ZnO films was found much higher ($>10^4$ Ω•cm), and should be good for the BRS device applications.

The polycrystalline ZnO thin films were grown by PEALD on (111) Pt/Ti/SiO_2/Si substrates. Diethylzinc (DEZn, 99.9999%) precursor was used for the deposition of ZnO. The

carrier gas and purging medium were 99.999% purity argon. During the growth, the pressure in the chamber was ~1 torr, and the substrate temperature was held at 150 °C. The flow rate of the carrier gas and the oxygen was 20 sccm and 40 sccm, respectively. A typical PEALD ZnO growth sequence is composed of 0.04 s of DEZn exposure, 6 s of Ar purging, 3 s of oxygen plasma exposure with RF power of 500 W, and 10 s of Ar purging. The ZnO films were ~60 nm thick for the devices which were grown by 250 cycles of the ALD process. X-ray diffraction (XRD) and Scanning Electron Microscope (SEM) were used to evaluate the crystal structure and morphology of the films. For electrical measurement, the top Al (100nm) electrode with a diameter of 200 μm was deposited by thermal evaporation using a metal mask to form the Al/ZnO/Pt sandwich device structure. The current–voltage (I–V) characteristics of the devices were measured using a semiconductor parameter analyzer (Agilent 4155 C) at room temperature in air.

Figure 1(a) shows the XRD spectrum of a ZnO thin film grown on the substrate. The (111) peak of the Pt bottom electrode and the (002) peak of the ZnO thin film can be clearly seen, indicating that the ZnO thin film has high c-axis orientation, largely attributed to the small lattice mismatch between the (002) plane of the ZnO film and Pt (111) plane. Figure 1(b) shows the SEM image of the cross-section of the as-fabricated ZnO/Pt/Ti/SiO_2/Si structure. The ZnO film has a polycrystal structure with a thickness of approximately 60 nm.

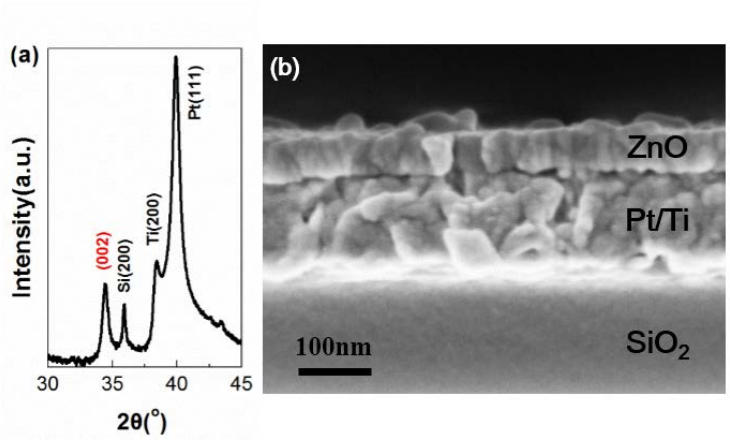

Fig. 1. (a) XRD pattern of a ZnO thin film deposited on a Pt/Ti/SiO_2/Si substrate. (b) The cross-section SEM image of the ZnO/Pt/Ti/SiO_2/Si structure.

The inset of Fig. 2 shows the schematic structure of the device and the scheme for electrical measurement. The DC voltage bias was applied to the top electrode (TE: Al) with the bottom electrode (BE: Pt) grounded during the measurements. It was found that the freshly-made devices always have a very high resistance, ~10^{12} Ω, and the devices do not exhibit any resistive switching behavior. An electroforming process is necessary to initiate the switching behavior for the devices. This is because the as-deposited ZnO films have high crystal quality with low density of defects, hence are high insulating. The electroforming process generates defects inside the ZnO layer, mostly by the thermally assisted electromigration of oxygen ions.[13] Figure 2 shows the typical bipolar resistive switching characteristics of the device after the forming process. The voltage bias was applied in a sweeping sequence of 1→2→3→4. The voltage sweeping from 0→3.5 V with a current compliance applied was used to set the device cell from the HRS to the LRS, while the opposite voltage sweep of 0→-2 V, with no current compliance, was used to reset the cell back to the HRS. The current compliance was set at 10 mA during the forming and set process to protect the device from permanent breakdown. However, if the current compliance was set to be 50 mA or higher for the forming process, the leakage current became very large during the voltage sweeping, and the devices changed to the LRS permanently.

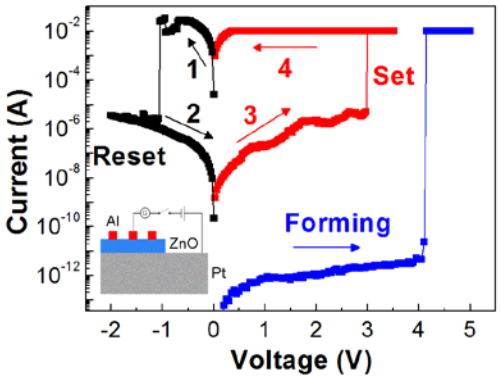

Fig. 2. Typical IV characteristics of Al/ZnO/Pt device. The inset shows the schematic structure for electrical measurement of Al/ZnO/Pt device. After the forming sweep (0→5V), a Reset-Set cycle is displayed. The resistance state is changed from LRS to HRS above the bias of -1V (reset) and changed from HRS to LRS above the bias of 3V (set).

To clarify the mechanism of bipolar resistive switching behavior, the typical I-V curve was replotted in double logarithmic plot. Figures 3(a) and 3(b) show the linear fitting of the I-V curve for both the negative and positive voltage sweep regions. When the device cell is switched to the LRS, the curves of log (I)-log (V) are linear with gradients near the unit ($I \propto V$), indicating that the I-V at the LRS is dominated by the Ohmic Law. At the HRS, the I-V is dominated by the Ohmic Law as well at low voltage region as the current and voltage are linearly correlated. But at high voltage region, the gradients of the log (I)-log (V) lines are around 2, i.e. the current is dependent of square of voltage applied ($I \propto V^2$). This result can be well explained by the typical trap-controlled space charge limited conduction (SCLC) injection. [6, 8, 14] The dominant conduction mechanisms of these devices at each voltage region are similar to the ZnO devices deposited by other methods. [6, 8, 15]

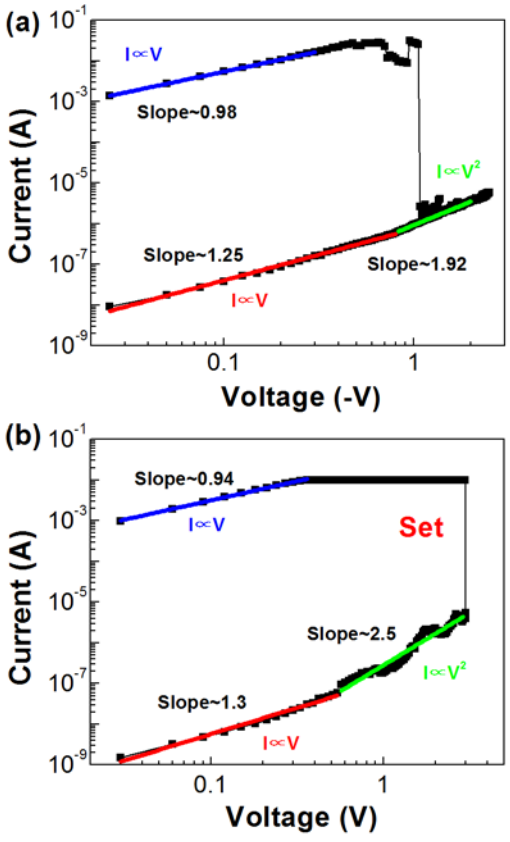

Fig. 3. Typical I–V curves of Al/ZnO/Pt device plotted in double logarithmic scale in negative (a) and

positive (b) sweeping voltage. The colorful lines show the fitting results.

A few mechanisms for resistive switching have been proposed with no convincing evidence.** The filamentary model has been widely accepted to explain the switching behavior for other ZnO-based resistive switching devices, and other TMO devices.[6, 16] After the forming process, defects are formed in the ZnO film. These may include oxygen vacancies, interstitial atoms or other defects , but the oxygen vacancies are believed to be the most important ones. [6, 16, 17] The oxygen ions migrate from the ZnO layer to/near the top electrodes at ** process. The oxygen vacancies are then generated in the ZnO film, forming the filament paths. Once the filaments connected the bottom electrode with the top electrode, the device cell is at the LRS. Whereas at the reset process, the oxygen ions near the top electrode are pushed back into the ZnO layer under the electric field, and the oxygen vacancies near the top electrode partially eliminated (neutralized) by reacting with the coming oxygen ions. The electrical paths (filaments) are broken, and the device cell is switched to the HRS. However there exist fragmented or disconnected filaments in the ZnO film even after reset due to the limited migration of the oxygen ions into the film, consequently the resistance of the HRS of the devices is always much lower than that of the as-made cells. Similarly, at the set process under a positive bias, the oxygen ions can migrate from the film to/near the top electrode, forming the filaments inside the ZnO film again. [16]

The endurance of the devices has been tested by switching the devices between the HRS and LRS for 50 cycles with the results shown in Fig. 4(a). The device cell showed a constant resistance for the LRS (~30Ω) and higher than 30 kΩ (10^4 Ω-10^7 Ω) resistance for the HRS during the cycling tests. The resistance ratio HRS/LRS is over 10^3 (10^3-10^6), which is higher than the Al/PVD-ZnO/Pt devices (10^2-10^3) [6-8], implying the high quality and low defect density of the ZnO films deposited by PEALD. The set voltage for our devices ranges from 1.2 to 3.6 V, whereas , that for Al/PVD-ZnO/Pt devices is from 0.47 to 2. 6V, lower than those of the PEALD-ZnO devices. Both the reset voltages are very low, about 0.5V. [6] Furthermore, similar BRS behaviors were obtained from cell to cell on the same wafer and from different wafers,

showed good repeatability and uniformity. However, the HRS resistance of the devices during the cycling tests varies significantly as shown in Fig. 4(a), and it is attributed to the difference in the free energies of oxide formation for Al and Zn. According to the research[6], the materials of the top electrode have a strong influence on the resistance. The Cr/ZnO/Pt devices have a smaller variation in resistances than the Al/ZnO/Pt devices shown here, and it is attributed to the smaller difference in free energies of oxide formation for Cr and Zn than that of Al and Zn. During the reset process, the top electrode cannot provide sufficient oxygen ions, some of the oxygen vacancies are left as they are near the top electrode, resulting in different resistance for each cycling test.[10,11] The endurance performance of the devices is expected to be improved significantly by scaling down the cell size or by improving the fabrication process.

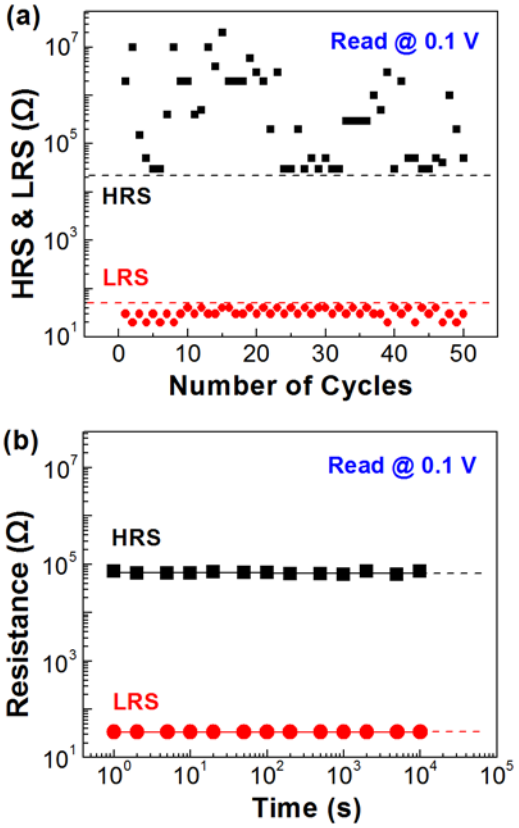

Fig. 4. (a) Endurance test for 50 consecutive Reset-Set cycles, readout at 0.1 V. (b) Retention tests of HRS and LRS after the Reset and Set, respectively, readout at 0.1 V.

The retention time of the Al/ZnO/Pt devices was measured at the HRS and LRS at room temperature at a voltage of 0.1 V as shown in Fig. 4(b). No electrical power was needed to maintain the resistances constant at the given states. Up to 10^4 s, the resistances of the HRS and LRS show no sign of deterioration at all, implying that the information stored in the devices can be kept much longer than 10^4 s. Therefore it can be concluded that the pure ZnO thin films deposited by PEALD can meet the requirement for ReRAM device application.

In summary, nanocrystalline ZnO thin films were grown by PEALD technique at low temperature, and were used to fabricate Al/ZnO/Pt resistive switching devices. Reversible resistive switching behavior of the devices has been obtained by electrically induced resistive switching between the LRS and HRS. The dominant conduction mechanisms of the LRS and HRS were Ohmic behavior and trap-controlled SCLC, respectively. The resistance ratio of the HRS to the LRS is larger than 10^3, and the resistances at both the states remain unchanged for the test up to 10^4 s, demonstrated the excellent potential of the PEALD-ZnO films for the applications in 3D ReRAM.

This work was supported by the Ministry of Science and Technology of China through the National Key Technology Support Program (No.2009BAG12A07), the National Natural Science Foundation of China (No. 61150110485), Zhejiang Province Innovation Group Program (No. 2011R09010) and Natural Science Foundation (Z1110168).

References

[1]R. Waser and M. Aono, Nat. Mater. **6,** 833 (2007).

[2]J. J. Yang, M. D. Pickett, X. M. Li, D. Ohlberg, D. R. Stewart, and R. S. Williams, Nat. Nanotechnol. **3,** 429 (2008).

[3]B. Magyari-Kope, M. Tendulkar, S. G. Park, H. D. Lee, and Y. Nishi, Nanotechnology **22,** 25402925SI (2011).

[4]Y. S. Kim, J. S. Kim, J. S. Choi, I. R. Hwang, S. H. Hong, S. O. Kang, and B. H. Park, Appl. Phys. Lett. **98,** 19210419 (2011).

[5]D. B. Strukov, G. S. Snider, D. R. Stewart, and R. S. Williams, Nature **453,** 80 (2008).

[6]W. Y. Chang, H. W. Huang, W. T. Wang, C. H. Hou, Y. L. Chueh, and J. H. He, J. Electrochem. Soc. **159**, 29 (2012).

[7]J. J. Ke, Z. J. Liu, C. F. Kang, S. J. Lin, and J. H. He, Appl. Phys. Lett. **99**, 19210619 (2011).
[8]C. Chen, F. Pan, Z. S. Wang, J. Yang, and F. Zeng, J. Appl. Phys. **111**, 0137021 (2012).
[9]D. Kim, H. Kang, J. M. Kim, and H. Kim, Appl. Surf. Sci. **257**, 3776 (2011).
[10]J. J. Yang, N. P. Kobayashi, J. P. Strachan, M. X. Zhang, D. Ohlberg, M. D. Pickett, Z. Y. Li, G. Medeiros-Ribeiro, and R. S. Williams, Chem. Mater. **23**, 123 (2011).
[11]H. B. Profijt, S. E. Potts, M. van de Sanden, and W. Kessels, J. Vac. Sci. Technol. A **29**, 0508015 (2011).
[12]R. L. Puurunen, J. Appl. Phys. **97**, 12130112 (2005).
[13]J. J. Yang, F. Miao, M. D. Pickett, D. Ohlberg, D. R. Stewart, C. N. Lau, and R. S. Williams, Nanotechnology **20**, 21520121 (2009).
[14]Z. B. Yan, Y. Y. Guo, G. Q. Zhang, and J. M. Liu, Adv. Mater. **23**, 1351 (2011).
[15]M. H. Tang, B. Jiang, Y. G. Xiao, Z. Q. Zeng, Z. P. Wang, J. C. Li, and J. He, Microelectronic Eng. **93**, 35 (2012).
[16]D. H. Kwon, K. M. Kim, J. H. Jang, J. M. Jeon, M. H. Lee, G. H. Kim, X. S. Li, G. S. Park, B. Lee, S. Han, M. Kim, and C. S. Hwang, Nat. Nanotechnol. **5**, 148 (2010).
[17]W. Y. Chang, C. S. Peng, C. H. Lin, J. M. Tsai, F. C. Chiu, and Y. L. Chueh, J. Electrochem. Soc., **158**, 872 (2011).